Recurrent *BCOR* Internal Tandem Duplication and *YWHAE-NUTM2B* Fusions in Soft Tissue Undifferentiated Round Cell Sarcoma of Infancy

Overlapping Genetic Features With Clear Cell Sarcoma of Kidney

Yu-Chien Kao, MD,† Yun-Shao Sung, MSc,† Lei Zhang, MD,† Shih-Chiang Huang, MD,†‡ Pedram Argani, MD,§ Catherine T. Chung, MD,‖ Nicole S. Graf, FRCPA,¶ Dale C. Wright, FHGSA, ARCPA, PhD,# Stewart J. Kellie, FRACP, MD,** Narasimhan P. Agaram, MD,† Kathrin Ludwig, MD,†† Angelica Zin, PhD,†† Rita Alaggio, MD,‡‡ and Cristina R. Antonescu, MD†*

Abstract: Soft tissue undifferentiated round cell sarcoma (URCS) occurring in infants is a heterogenous group of tumors, often lacking known genetic abnormalities. On the basis of a t(10;17;14) karyotype in a pelvic URCS of a 4-month-old boy showing similar breakpoints with clear cell sarcoma of kidney (CCSK), we have investigated the possibility of shared genetic abnormalities in CCSK and soft tissue URCS. Most CCSKs are characterized by *BCOR* exon 16 internal tandem duplications (ITDs), whereas a smaller subset shows *YWHAE-NUTM2B*/*E* fusions. Because of overlapping clinicopathologic features, we have also investigated these genetic alterations in the so-called primitive myxoid mesenchymal tumor of infancy (PMMTI). Among the 22 infantile URCSs and 7 PMMTIs selected, RNA sequencing was performed in 5 and 2 cases, with frozen tissue, respectively. The remaining cases with archival material were tested for *YWHAE-NUTM2B*/*E* by fluorescence in situ hybridization (FISH) or reverse transcription-polymerase chain reaction (RT-PCR), and *BCOR* ITD by PCR. A control group of 4 CCSKs and 14 URCSs in older children or adults without known gene fusion and 20 other sarcomas with similar histomorphology or age at presentation were also tested. A *YWHAE-NUTM2B* fusion was confirmed in the index case by FISH and RT-PCR, whereas *BCOR* ITD was lacking. An identical *YWHAE-NUTM2B* fusion was found in another URCS case of a 5-month-old girl with a back lesion. The remaining cases and control group lacked *YWHAE* gene rearrangements; instead, consistent *BCOR* ITDs, similar to CCSK, were found in 15/29 (52%) infantile sarcoma cases (9/22 infantile URCS and 6/7 PMMTI). In the control cohort, *BCOR* ITD was found only in 3 CCSK cases but not in the other sarcomas. Histologically, URCS with both genotypes and PMMTI shared significant histologic overlap, with uniform small blue round cells with fine chromatin and indistinct nucleoli. A prominent capillary network similar to CCSK, rosette structures, and varying degree of myxoid change were occasionally seen. *BCOR* ITD–positive tumors occurred preferentially in the somatic soft tissue of the trunk, abdomen, and head and neck, sparing the extremities. RNAseq showed high *BCOR* mRNA levels in *BCOR* ITD–positive cases, compared with other URCSs. In summary, we report recurrent *BCOR* exon 16 ITD and *YWHAE-NUTM2B* fusions in half of infantile soft tissue URCS and most PMMTI cases, but not in other pediatric sarcomas. These findings suggest a significant overlap between infantile URCS and CCSK, such as age at presentation, histologic features, and genetic signature, thus raising the possibility of a soft tissue counterpart to CCSK.

Key Words: small blue round cell tumor, undifferentiated sarcoma, infantile, BCOR ITD, YWHAE, clear cell sarcoma kidney, primitive mesenchymal myxoid tumor of infancy

(*Am J Surg Pathol* 2016;00:000–000)

From the *Department of Pathology, Shuang Ho Hospital, Taipei Medical University, Taipei; ‡Department of Anatomical Pathology, Chang Gung Memorial Hospital, Chang Gung University College of Medicine, Taoyuan, Taiwan; †Department of Pathology, Memorial Sloan Kettering Cancer Center, New York, NY; §Departments of Pathology and Oncology, Johns Hopkins University School of Medicine, Baltimore, MD; ‖Department of Paediatric Laboratory Medicine, Division of Pathology, The Hospital for Sick Children, Toronto, ON, Canada; Departments of ¶Histopathology; **Pediatric Oncology, University of Sidney, The Children's Hospital at Westmead; #Department of Cytogenetics, Sydney Genome Diagnostics, Sydney, NSW, Australia; ††Institute of Pediatric Research Citta'della Speranza; and ‡‡Pathology Unit, Department of Medical and Diagnostic Sciences and Special Therapies, University of Padua, Padua, Italy.

Conflicts of Interest and Source of Funding: Supported in part by: P50 CA140146-01 (C.R.A.); P30-CA008748 (C.R.A.); Kristen Ann Carr Foundation (C.R.A.), Cycle for Survival (C.R.A.). The authors have disclosed that they have no significant relationships with, or financial interest in, any commercial companies pertaining to this article.

Correspondence: Cristina R. Antonescu, MD, Pathology Department, Memorial Sloan Kettering Cancer Center, 1275 York Ave, New York, NY, 10065 (e-mail: antonesc@mskcc.org).

Supplemental Digital Content is available for this article. Direct URL citations appear in the printed text and are provided in the HTML and PDF versions of this article on the journal's Website, www.ajsp.com.

Undifferentiated round cell sarcoma (URCS) is a heterogenous group of tumors composed of tumor cells with monomorphic round nuclei and scant cytoplasm, which usually lacks a known recurrent genetic abnormality and remains unclassified by currently established tumor entities.[1] On the basis of an index case of a 4-month-old boy with a pelvic round cell sarcoma harboring an identical *YWHAE-NUTM2B* fusion to clear cell sarcoma of kidney (CCSK), we further investigated the possibility of shared genetic abnormalities between CCSK and infantile soft tissue URCS.

CCSK is an aggressive renal sarcoma of young childhood. The classic histologic appearance of CCSK is composed of monotonous round cells with fine to open chromatin, indistinct nucleoli, and delicate chicken-wire capillaries separating the tumor cells into nests. A wide spectrum of morphologies has also been described, including a myxoid background, sclerosing stroma, epithelioid pattern with acinar or rosette-like structures, areas of spindling, storiform growth pattern, rare rhabdoid cytoplasmic inclusions, etc.[2] As there have been no specific confirmatory ancillary tests for CCSK, the diagnosis relies largely on the histomorphology and anatomic presentation in the kidney. Only rare cases of extrarenal CCSK either occurring in other viscera (ileum, ovary)[2–4] or soft tissues[2,5,6] have been reported. However, recent studies have identified recurrent genetic abnormalities in CCSK, characterized by either internal tandem duplication (ITD) in exon 16 of *BCOR* in the majority of cases or the presence of t(10;17)(q22.3;p13.3) translocation resulting in *YWHAE-NUTM2B*/*E* fusions in a smaller subset of cases.[7,8] These 2 genetic alterations appear to be mutually exclusive.[9] With these recent advances in the genetic signatures of CCSK, molecular studies can be applied to further investigate the relationship between CCSK and infantile soft tissue URCS.

Another tumor that shares a similar age at presentation and cytomorphology of uniform round to spindle cells is the so-called primitive myxoid mesenchymal tumor of infancy (PMMTI). PMMTI is a soft tissue sarcoma occurring almost exclusively in the trunk, extremities, and head and neck of infants and is histologically composed of sheets of primitive round to spindle cells, a delicate vascular network, and a variably myxoid background.[10] The genetic alterations of PMMTI are unknown. Considering the overlapping clinicopathologic features, we hypothesized that PMMTI shares similar genetic abnormalities with URCS and CCSK and thus have investigated the presence of *BCOR* ITD and *YWHAE-NUTM2B*/*E* fusions in a group of PMMTIs.

MATERIALS AND METHODS

Patient Selection

The index case was a 4-month-old boy with a pelvic tumor, measuring 8.1 cm, extending to the right retroperitoneum and lumbosacral spinal canal. Computed tomography scan showed that the tumor indented the inferior pole of the right kidney without involving it. The tumor was biopsied, and the morphology showed a small blue round cell tumor with round to ovoid nuclei, fine chromatin, indistinct nucleoli, and frequent mitoses (Fig. 1A). A delicate arborizing capillary network was not identified. Conventional cytogenetics found an apparently 3-way reciprocal translocation t(10;17;14)(q22.1;p13.3;q24) (Fig. 1B), involving similar regions of chromosome 10 and 17 as reported previously in CCSK.[8]

Aiming for cases of similar age at diagnosis and histology, we selected patients younger than 1 year of age (infants), diagnosed with a round cell sarcoma, undifferentiated or unclassified sarcoma, or PMMTI, from the consultation archives of 3 of the senior authors (C.T.C., R.A., C.R.A.). All cases were then tested to exclude known fusion genes, such as *EWSR1*, *FUS*, *CIC*, *BCOR*, *ETV6-NTRK3*, by fluorescence in situ hybridization (FISH) or reverse transcription-polymerase chain reaction (RT-PCR). Together with the index case, 29 cases were identified, including 22 URCS and 7 PMMTI cases (Table 1). Representative hematoxylin and eosin–stained slides were reviewed, and the following histologic features were recorded: including cytomorphology (round, spindle), mitotic activity, necrosis, vascular network, rosette formation, fibrous septa, and type of stroma (myxoid, sclerotic). Immunohistochemical stains were also reviewed, and follow-up information was obtained from the referring pathologists. Two of the PMMTI cases (PMMTI1 and 2) have been previously reported.[10]

To further investigate the distribution of these genetic abnormalities among URCS of different age groups and across different tumor entities prevalent in young children, we also included as controls: 14 cases of noninfantile URCS, 2 Ewing sarcomas, 3 *CIC-DUX4*-positive round cell sarcomas, 3 *BCOR-CCNB3*-positive round cell sarcomas, 1 *BCOR-MAML3* round cell sarcoma,[11] 8 rhabdomyosarcomas (3 embryonal rhabdomyosarcoma, 5 spindle cell/sclerosing rhabdomyosarcoma), 2 malignant ectomesenchymomas, and 1 myofibromatosis. Four CCSK cases were included as positive controls. This study was approved by the institutional review board at all participating institutions.

Fluorescence In Situ Hybridization

FISH for *YWHAE* gene break-apart was performed on 4-μm-thick formalin-fixed paraffin-embedded (FFPE) tissue sections. If the result was positive, FISH for *NUTM2B*/*E* break-apart was subsequently performed. Custom probes were made by bacterial artificial chromosomes (BAC) clones (Supplementary Table 1, Supplemental Digital Content 1, http://links.lww.com/PAS/A349) flanking the *YWHAE* or *NUTM2B*/*E* gene according to the UCSC genome browser (http://genome.ucsc.edu) and obtained from BACPAC sources of Children's Hospital of Oakland Research Institute (Oakland, CA; http://bacpac.chori.org). The BAC clones were labeled with fluorochromes by nick translation and validated on normal metaphase chromosomes. The slides were deparaffinized, pretreated, and hybridized with denatured probes. After overnight incubation, the slides were then washed, stained with DAPI, mounted with antifade, and examined on a Zeiss fluorescence microscope (Zeiss Axioplan, Oberkochen, Germany) controlled by Isis 5 software (Metasystems). Of the 200 cells counted,

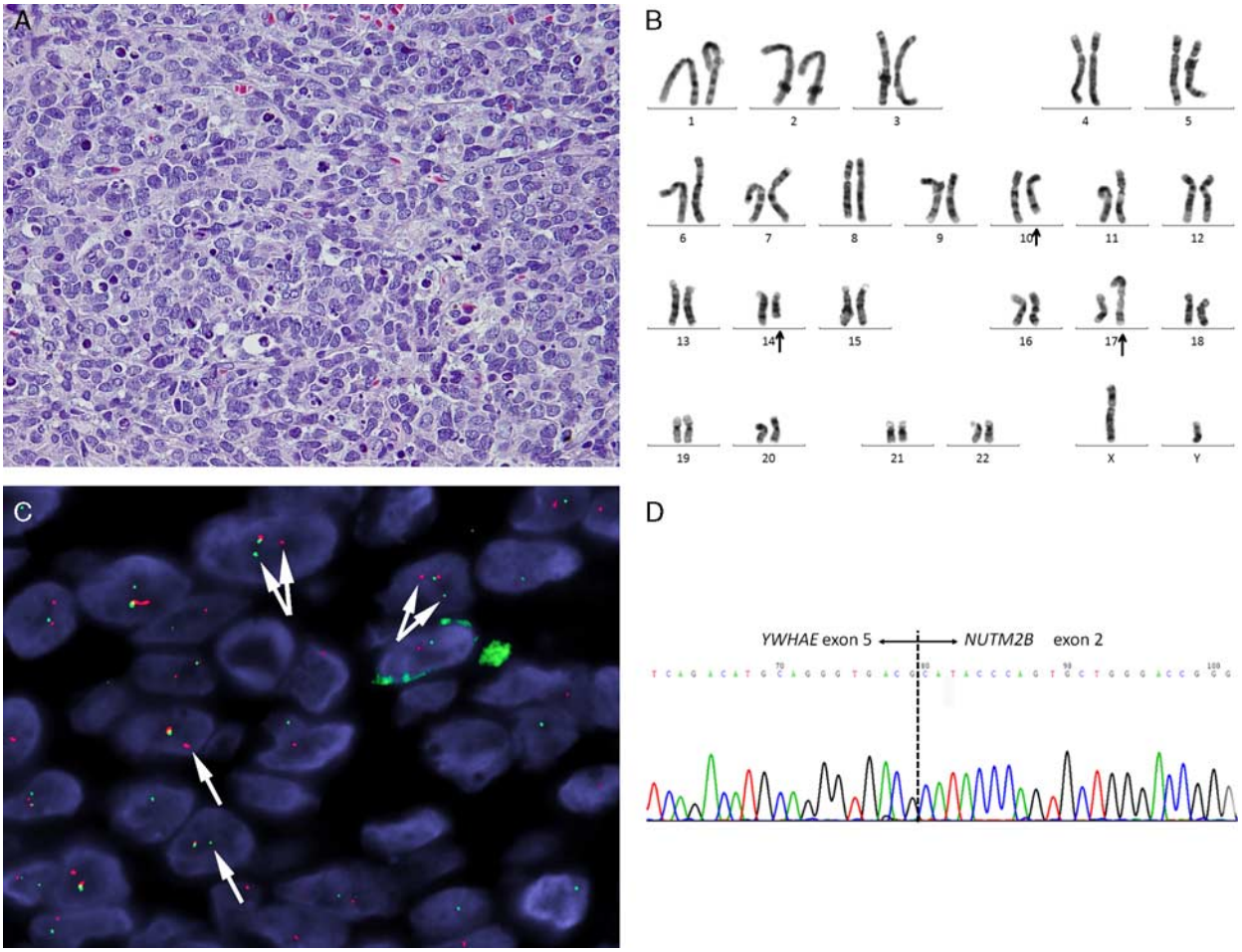

FIGURE 1. The index URCS case with *YWHAE-NUTM2B* fusion. Diffuse sheets of monotonous round cells with fine chromatin, indistinct nucleoli, frequent apoptosis, and occasional mitoses (A, hematoxylin and eosin). Representative karyotype showing a 3-way translocation t(10;17;14)(q22.1;p13.3;q24) indicated by the arrows (B). FISH showing *YWHAE* rearrangement, with break-apart green (telomeric) and red (centromeric) signals (C, white arrows). Sanger sequencing of RT-PCR product demonstrating *YWHAE* exon 5 fused to *NUTM2B* exon 2 (D).

>20% of tumor nuclei with break-apart signals were considered as positive.

RNA Sequencing

RNA sequencing (RNAseq) was performed in cases with available fresh frozen tumor tissues, including 7 cases of infantile sarcomas (5 URCS [URCS# 2, 3, 4, 5, 8] and 2 PMMTI [PMMTI# 1, 2]), 2 noninfantile URCS, 1 Ewing sarcoma, 1 *BCOR-MAML3*-positive round cell sarcoma, 2 ectomesenchymomas, 1 myofibromatosis, and 5 rhabdomyosarcomas. Total RNA was extracted by RNeasy Plus Mini (Qiagen) from fresh frozen tumor tissues. The mRNA was isolated with oligo(dT) magnetic beads from total RNA (2 μg) and fragmented by incubation at 94°C for 2.5 minutes in a fragmentation buffer (Illumina). To reduce the inclusion of artifact chimeric transcripts into the sequencing library, an additional gel size–selection step was introduced before the adapter ligation step. The adaptor ligated library was then enriched by PCR for 15 cycles and purified. The library was sized and quantified using DNA1000 kit (Agilent) on an Agilent 2100 Bioanalyzer according to the manufacturer's instructions. Paired-end RNAseq at read lengths of 50 or 51 bp was performed with the HiSeq 2000 (Illumina). All reads were independently aligned with STAR (ver 2.3)[12] and TopHat2 (ver 2.0.14)[13] against the human reference genome (hg19). On the basis of the known genetic abnormalities reported in CCSK,[7,8] the reads were also investigated manually for *YWHAE-NUTM2B/E* fusion and *BCOR* ITD. The mRNA expression of *BCOR* and PEA3 family genes, including *ETV1*, *ETV4*, and *ETV5*, was analyzed and compared with other sarcomas.

Reverse Transcription-Polymerase Chain Reaction for *YWHAE-NUTM2B/E*

RT-PCR was performed to validate the *YWHAE-NUTM2B/E* fusion observed by FISH or RNAseq in 2 cases. In addition, 3 cases negative for *YWHAE-NUTM2B/E* fusion by RNAseq were also included as

TABLE 1. Clinicopathologic Features and Genetic Abnormalities of Infantile URCS and PMMTI

Case	Age/Sex	Location	Morphology			*YWHAE-NUTM2B/E*	BCOR ITD	Follow-up
			Rosette	Arb Vessels	Myxoid			
URCS1	4 mo/M	Pelvic	−	−	−	+*†‡	−‡	DR, DOD (3 mo)
URCS2	5 mo/F	Back	−	E	−	+†‡§	−‡§	NA
URCS3	23 d/M	Back	−	E	−	−‡§	+‡§	NA
URCS4	8 d/F	Buttock	+	−	−	−†‡§	+‡§	LR, DOD (26 mo)
URCS5	3 mo/F	Jaw	+	−	Foc	−†‡§	+‡§	NED (41 mo)
URCS6	3 mo/M	RP	−	−	E	−†	+‖	NA
URCS7	11 mo/M	Chest wall	−	−	−	−†	+‖	NA
URCS8	2 wk/F	Chest wall	−	E	E	−†	+§‖	NA
URCS9	10 d/M	Neck	−	−	E	−†	+‖	LR (4 mo)
URCS10	5 mo/M	RP/pelvic	−	Foc	Foc	−†	+‖	NA
URCS11	10 mo/M	Paravertebral	−	E	−	−†	+‖	NA
URCS12	1 mo/M	Para-anal	−	−	−	−†	−‖	NA
URCS13	10 d/M	Tibia, fibula	−	−	−	−†	−‖	NA
URCS14	6 mo/M	Paratesticular	−	−	Foc	−†	−‖	NA
URCS15	1 y/F	Orbit	−	−	−	−†	−‖	NA
URCS16	1 y/F	Shoulder	−	−	−	−†	−‖	NA
URCS17	1 y/M	Mandible	−	−	Foc	−†	−‖	NA
URCS18	1 y/F	Forearm	−	−	−	−†	−‖	NA
URCS19	1 mo/F	Neck	−	−	−	−†	−‖	NA
URCS20	6 mo/F	Pelvic	−	−	−	−†	−‖	NA
URCS21	1 y/F	Back	−	Foc	−	−†	−‖	NA
URCS22	9 mo/F	Ankle	−	−	−	−†	−‖	NA
PMMTI1	2 mo/M	Paraspinal	−	Foc	E	−§	+§‖	DR (6 mo)
PMMTI2	5 mo/M	Larynx	−	−	Foc	−§	+§‖	LR, DOD (5 y)
PMMTI3	9 mo/M	Abdominal wall	−	E	E	−†	+‖	LR (5 mo)
PMMTI4	6 mo/M	RP	−	E	Foc	−†	+‖	NA
PMMTI5	10 mo/F	Abdominal cavity	−	E	Foc	−†	+‖	NA
PMMTI6	4 mo/F	Paravertebral	−	E	Foc	−†	+‖	NA
PMMTI7	1 y/M	Thigh	−	E	Foc	−†	−‖	NA

*By conventional cytogenetics.
†By FISH.
‡By RT-PCR.
§By RNAseq.
‖By genomic PCR.
Arb indicates arborizing; DOD, dead of disease; DR, distant recurrence (metastasis); E, extensive; F, female; Foc, focal; LR, local recurrence; M, male; NA, not available; NED, no evidence of disease; RP, retroperitoneum.

negative control. RNA was extracted from fresh frozen tissues by RNeasy Plus Mini (Qiagen) or from FFPE tissues by Trizol reagent (Invitrogen). The primers were designed with forward primer at exon 5 of *YWHAE* (5′-GCAGAA CTGGATACGCTGAGTGAAG-3′) and reverse primer at exon 2 of *NUTM2B/E* (5′-GTGTTGTGTGTCCACC TCCCCTAC-3′ for fresh frozen tissue; 5′-GGCTTCCAAC GTCTTTGTCCAG-3′ for FFPE tissue), on the basis of the fusion junction reported previously.[8] As the 2 nearby *NUTM2B* and *NUTM2E* genes share significant homology, we used a consensus primer for RT-PCR screening, the 2 gene transcripts differing by 1 nucleotide.[8] RT-PCR was performed using SuperScript III First-Strand Synthesis System (Invitrogen) and Advantage 2 PCR kit (Clontech, Mountain View, CA) at an annealing temperature of 66.0°C for 35 cycles. The PCR products were then analyzed by agarose gel electrophoresis and Sanger sequencing.

PCR for *BCOR* Exon 16 ITD

Depending on the material available, genomic PCR or RT-PCR was performed to detect *BCOR* ITD. In 1 of the CCSK cases, non-neoplastic kidney parenchyma was available and also tested. Genomic DNA was extracted from FFPE tissues by QIAamp DNA FFPE Tissue Kit (Qiagen), except in 5 cases (URCS 1 to 5), where complementary DNA was synthesized as described above. Primer sequences were designed to target the last exon (exon 16) of *BCOR* (Fwd-1: 5′-GTCCTCCCGCA TATTTCGC-3′ or Fwd-2: 5′-GACCTGGAAGCCTT CAACCC-3′ and Rev: 5′-CAAGCTGGACCCACCA TGTAC-3′). PCR was performed using Advantage 2 PCR kit at an annealing temperature of 65.2°C (Fwd-1) or 66.5°C (Fwd-2) for 38 cycles. The PCR products were then analyzed by agarose gel electrophoresis. Amplicons with size larger than wild type were subsequently sequenced using the Sanger method to confirm the presence of ITD.

Comparison of *BCOR* ITD–positive Sarcomas Gene Expression Profile With CCSK and *BCOR-CCNB3*–positive Sarcomas

For the gene expression analysis, all genome-wide RPKM values were quantile normalized, and signal intensities were log2 transformed.[14] The transcriptional profile of the 7 infantile sarcomas (5 URCS, 2 PMMTI) was compared with the gene expression of a large spec-

trum of sarcomas (n = 120) available on the RNAseq platform. A differentially expressed gene list was obtained by using a log2-Fold-Change threshold of positive 1.3 or negative 5 and a 0.01 false discovery rate (FDR).

We next set out to compare the gene expression signature of *BCOR* ITD and *YWHAE* fusion–positive URCS/PMMTI (described above) with the published transcriptional profile of CCSK and other *BCOR* fusion–positive sarcomas. The previously reported gene expression data from 22 CCSKs (20 *BCOR* ITD and 2 *YWHAE-NUTM2B/E*-positive) and a control group of fetal (n = 4) and adult kidney (n = 6), available on the Illumina HumanHT-12 V4.0 beadchip platform, GEO (GSE49972), were downloaded[15] and analyzed using a log2-Fold-Change of negative 5 or positive 1.7 and 0.05 FDR as statistical thresholds. The differentially expressed gene list obtained was then probe-matched to the RNA-seq annotation (hg19) for comparison.

We then obtained the publicly available expression data of 10 *BCOR-CCNB3* fusion–positive round cell sarcomas from GEO (GSE34800)[16] and a control group of normal tissues from GEO (GSE7307) tested on Affymetrix Human Genome U133A Plus 2 platform. For data analysis, robust multiarray average normalization was performed, including background correlation, quantile normalization, and median polish summary methods.[17] Subsequent analysis was carried out with signal intensities that were log2 transformed to remove biases based on signal expression values. Statistical *t* test and FDR were performed to identify differentially expressed gene list. Differentially expressed gene profile was obtained by the threshold of log2 negative 5 or positive 2.5 with 0.01 FDR, followed by probe-matched to the RNAseq annotation (hg19).

After the differentially expressed gene list of each tumor entity was defined, we selected a common core gene set, shared by the 3 tumor types by Venn diagram, and used it for gene set enrichment analysis (GSEA) and complete-linkage hierarchical clustering for each entity. For GSEA, the gene lists were ranked in the order of signal-to-noise ranking metric between the tumor types (*BCOR* ITD–positive URCS/PMMTI, *BCOR* ITD–positive CCSK, and *BCOR-CCNB3* round cell sarcoma) and the control group available in each platform as mentioned above.

RESULTS

YWHAE-NUTM2B Fusion Is a Rare Event in Infantile URCS

The clinicopathologic and molecular results of the 29 infantile URCS/PMMTI cases are summarized in Table 1. Break-apart FISH assay confirmed *YWHAE* and *NUTM2B/E* gene rearrangements in the index case (URCS1) (Fig. 1C). RT-PCR and subsequent direct sequencing showed fusion of exon 5 of *YWHAE* to exon 2 of *NUTM2B* (Fig. 1D). On the basis of the RNAseq data, we identified a second URCS (5-mo-old girl, back soft tissue mass) with identical *YWHAE-NUTM2B* fusion (URCS2). This result was further confirmed by RT-PCR and FISH. FISH screening of the remaining infantile URCS/PMMTI and control cases showed no additional cases with break-apart abnormalities in *YWHAE*.

Morphologically, both cases were composed of small round tumor cells with fine to open chromatin, indistinct nucleoli, and scant cytoplasm. A prominent branching vascular network reminiscent of CCSK was present in URCS2 (Fig. 2A). There was no obvious myxoid stroma or rosette formation. Lymphovascular invasion was noted in URCS2. CD99 immunostains were negative in both cases. The index case developed brain metastasis and died of disease 3 months after diagnosis. URCS2 was a recent case with no follow-up information available to date.

BCOR ITD Is the Most Frequent Genetic Event in Infantile Soft Tissue URCS

In the remaining 4 URCS cases with RNAseq results, all of them were found to have *BCOR* exon 16 ITD, which was subsequently confirmed by RT-PCR or genomic PCR. Furthermore, 5 additional URCS cases were positive for *BCOR* ITD by genomic PCR from FFPE tissues. Thus a total of 9 infantile URCS of 22 tested (41%) were positive for *BCOR* ITD (Table 1 and Fig. 3A). The duplicated sequence from the *BCOR* exon 16 varied in size (66 to 99 bp) and genomic position; 8 of the positive cases encompassed 4 different variants (Fig. 3A), whereas the ITD variant was undetermined in 1 case.

Among the patients with *BCOR* ITD–positive tumors, there were 6 boys and 3 girls (male to female ratio, 2:1), with an age at presentation ranging from 8 days to 11 months old. The tumors occurred in the somatic soft tissue of trunk (5), pelvis/retroperitoneum (2), and head and neck (2). Morphologically, most cases were composed of sheets or lobules of monotonous small round cells with fine chromatin. The characteristic delicate arborizing capillary network was observed diffusely in 3 cases and focally in 1 (Fig. 2B). Two cases had cellular fibrous septa as seen in CCSK (Fig. 2C). Variable degree of myxoid stromal change was noted in 5 cases, including 1 with extensive cystic change (Fig. 2D). Two cases showed well-formed rosette structures (Fig. 2E). Most cases showed scant cytoplasm, but clear or vacuolated cytoplasm was noted in 3 cases (diffuse in 2, focal in 1) (Fig. 2F), and appeared to coalesce into microcystic spaces in 1 case. Focal multinucleated giant cells with smudged nuclei were seen in 1 case (URCS4, second recurrence). Most of the cases were mitotically active (> 4/10 HPFs in 66% cases), except for cases with extensive myxoid change, which had lower mitotic counts. Some showed abundant karyorrhexis. Lymphovascular invasion was noted in 1 case. CD99 membranous immunostaining was positive in 3 of 6 cases (2 diffuse, 1 focal). There was no obvious association between ITD variants and tumor location, sex, degree of myxoid

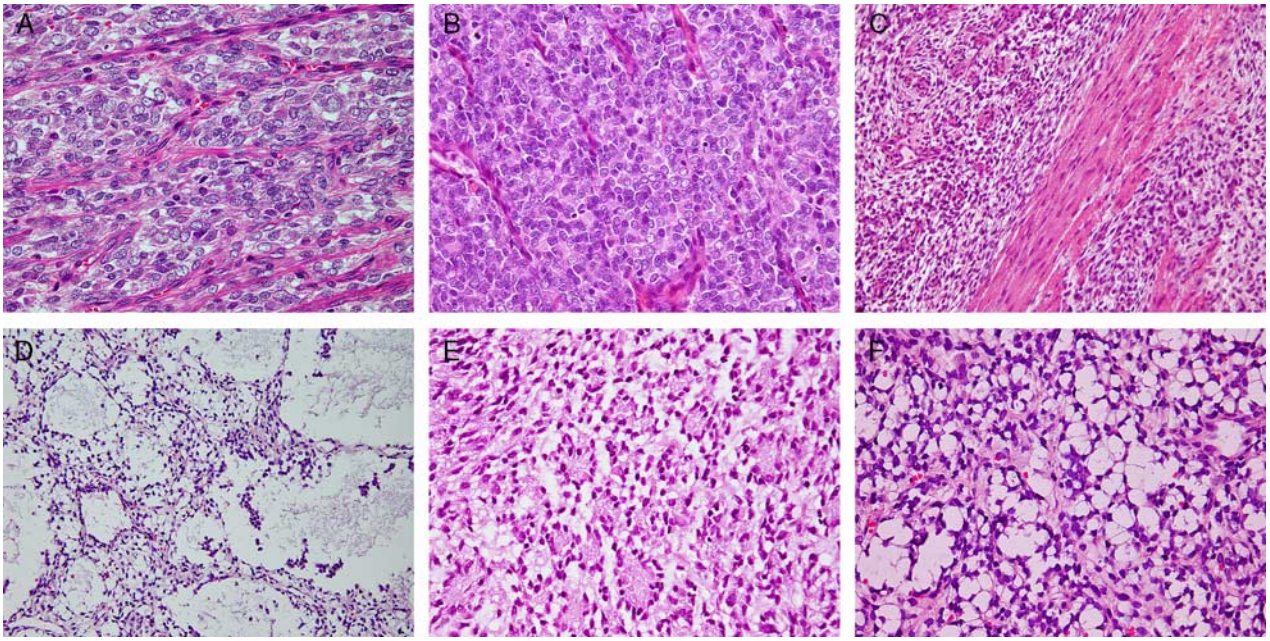

FIGURE 2. Histology of soft tissue URCS with *YWHAE-NUTM2B* fusion (A) or *BCOR* ITD (B–F). Second case with *YWHAE-NUTM2B* fusion showing delicate arborizing vascular network reminiscent to CCSK (A, URCS2). *BCOR* ITD URCS showing a prominent capillary network (B, URCS3); cellular fibrous septa (C, URCS3); uniform round to ovoid tumor cells (B); extensive myxoid stroma and cystic spaces (D, URCS6); rosette formation (E, URCS5), and vacuolated cytoplasm (F, URCS6).

change, or the presence of a delicate vascular pattern. Both cases with prominent rosette formation had the same ITD subtype. Follow-up information was available in 3 patients: 1 experienced 4 locoregional recurrences and succumbed to the disease 26 months after diagnosis; 1 had a local recurrence 4 months after diagnosis; the third has shown no evidence of disease 41 months after diagnosis.

PMMTIs Share Similar *BCOR* ITD With Soft Tissue Infantile URCS and CCSK

From the 7 PMMTI cases examined, all except 1 case (86%) were found to be positive for *BCOR* ITD, 2 by RNAseq sequencing and 4 by genomic PCR. There were 4 *BCOR* ITD variants identified (63 to 120 bp, Fig. 3A), including 1 identical to URCS, whereas the ITD variant could not be determined in 1 case.

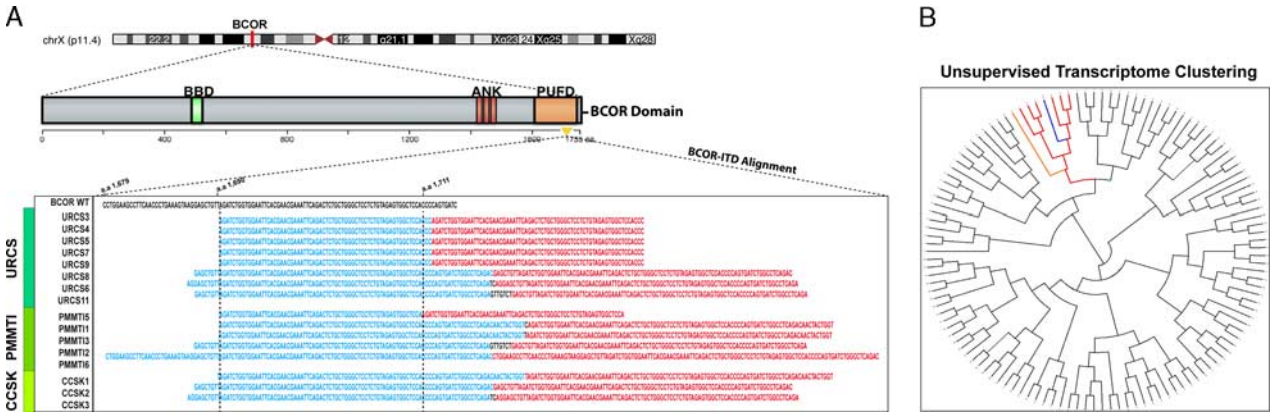

FIGURE 3. Spectrum of *BCOR* ITD variants in URCS, PMMTI, and CCSK samples. A, Schematic diagram showing the location of *BCOR* on chromosome Xp11.4, protein domains of BCOR, the location of the duplicated sequences on PUFD domain, and the ITD subtypes among URCS, PMMTI, and CCSK. Compared with wild-type *BCOR*, the original and duplicated sequences are shown in blue and red, respectively. The intervening sequences in black indicate insertions; however, all ITD variants are in-frame. The common region of duplicated sequence is indicated by vertical dot lines. B, By unsupervised clustering, the URCS/PMMTI with *BCOR* ITD (red), *YWHAE-NUTM2B* fusion (blue), and *BCOR-MAML3* fusion (orange) grouped together in a distinct cluster from other sarcomas available on the RNAseq. ANK indicates ankyrin repeat; BBD, BCL-6 binding domain; PUFD, PCGF Ub-like fold discriminator.

The 6 PMMTI cases harboring *BCOR* ITD affected patients between 2 and 10 months old, with equal sex distribution. The location of the tumors included soft tissue of trunk (3), abdomen/retroperitoneum (2), and larynx (1). Tumor sizes ranged from 2.5 to 5.5 cm in the 3 cases (PMMTI1, 2, 6) with available information. There was significant morphologic overlap with CCSK and URCS, but the PMMTI cases showed more prominent myxoid stroma. The tumor cells were predominantly round to ovoid (Fig. 4A), less frequently stellate (2 cases, Fig. 4B), and rarely spindled (1 case, Fig. 4C). Chicken-wire branching vasculature was also present in 5 cases, being diffuse in 4 and focal in 1 (Fig. 4D). One case also showed the presence of cellular fibrous septa (Fig. 4E), similar to that seen in CCSK and some cases of infantile URCS. Vacuolated cytoplasm or rhabdoid morphology was observed in 2 cases each (Figs. 4F, G). One case had lymphovascular invasion. CD99 staining was not performed in these cases, and no additional material was available for further immunohistochemical stains. One patient died of disease 5 years after diagnosis, whereas the other 2 patients are alive with disease after a short follow-up available (5 and 6 mo, respectively; Table 1).

The only PMMTI case negative for *BCOR* ITD occurred in a 21-month-old boy, who developed a gradually enlarging thigh mass since he was 17 months old. Histologically, it was composed of ovoid to stellate tumor cells in a myxoid background accompanied by a delicate vasculature throughout, almost indistinguishable from other PMMTIs, except that the chromatin pattern was slightly more clumped (Fig. 4H).

No *YWHAE-NUTM2B/E* Fusions or *BCOR* ITDs Are Identified in Other Infantile or Noninfantile Sarcomas

None of the other tumors included in the control group were found to share these genetic abnormalities, as investigated by FISH for *YWHAE* rearrangement, PCR

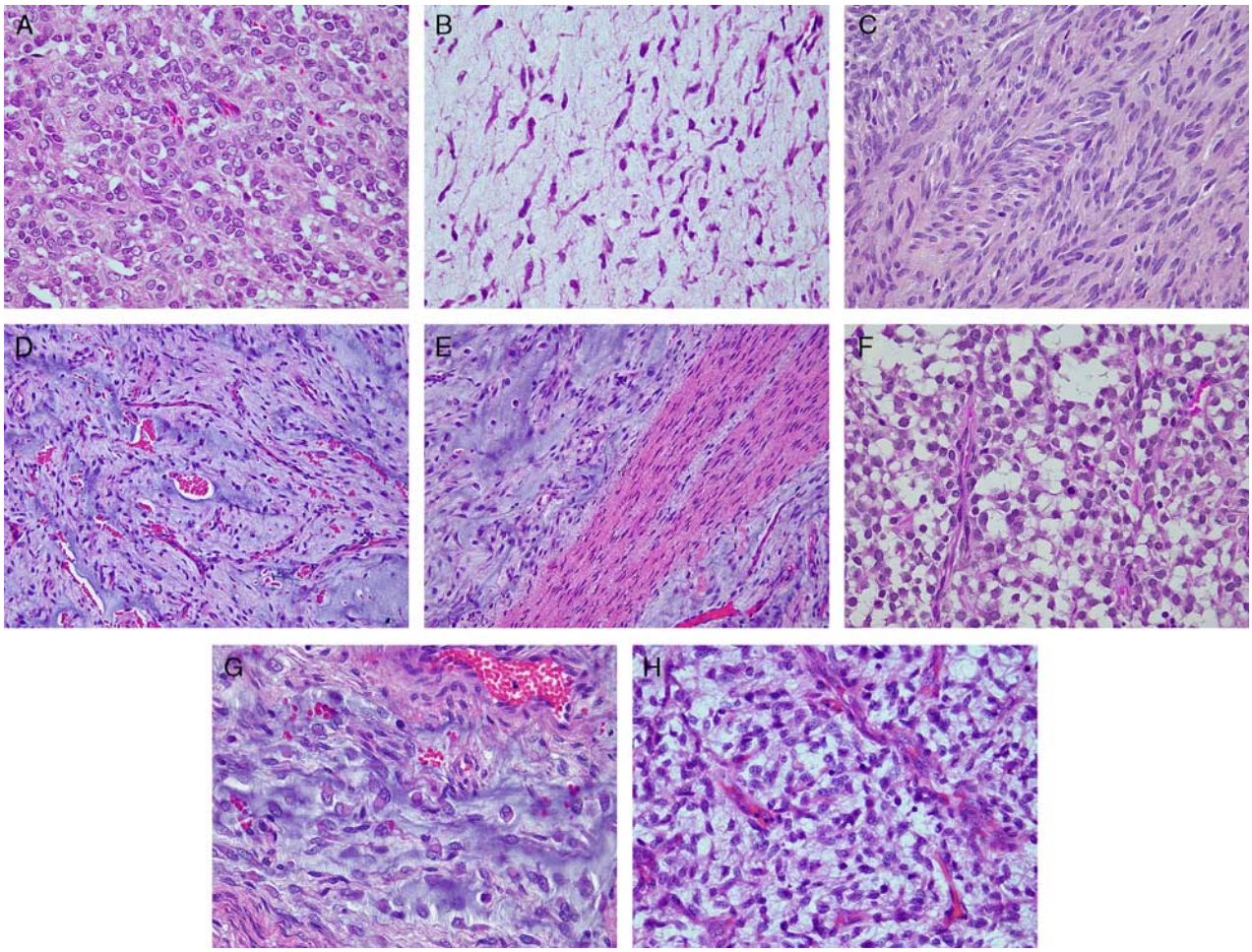

FIGURE 4. Morphologic spectrum of PMMTI. The PMMTIs were associated with a monomorphic cytomorphology, ranging from round (A, PMMTI6), stellate (B, PMMTI6), to spindle (C, PMMTI2). Overlapping histologic features with *BCOR* ITD URCS and CCSK were noted, including rich vascular network (D, PMMTI6) and cellular fibrous septa (E, PMMTI3). Other features included occasional cytoplasmic vacuoles (F, PMMTI6) or rhabdoid cells (G, PMMTI). The only PMMTI lacking *BCOR* ITD showed ovoid to stellate tumor cells, with slightly clumped chromatin and myxoid stroma (H, PMMTI7).

for *BCOR* ITD, and/or RNAseq. As expected, 3 of 4 CCSKs were positive for *BCOR* ITD, but none showed *YWHAE* gene rearrangement. The non-neoplastic renal parenchyma of 1 CCSK case was negative for *BCOR* ITD in contrast to the adjacent tumor, excluding a constitutional genetic change. The *BCOR* ITD variants were different from each other in the 3 CCSK cases, including 1 previously unreported variant (Fig. 3A).[7,9,18,19]

Upregulation of *BCOR* mRNA Is a Common Feature of URCS/PMMTI and CCSK With Either *BCOR* ITD, *YWHAE-NUTM2B*, or *BCOR*-related Fusions

By RNAseq, all *BCOR* ITD–positive tumors (4 URCS, 2 PMMTI) showed a very high level of *BCOR* mRNA expression (Fig. 5B). The high *BCOR* expression was not restricted to the last exon, where the ITD occurred, but spanned throughout the entire transcript (data not shown). An intermediate level of BCOR overexpression was also noted in the *YWHAE-NUTM2B*-positive URCS and in the *BCOR-MAML3*-positive round cell sarcoma but not in other sarcomas available on our RNAseq platform (Fig. 5B). Furthermore, *BCOR* upregulation was also identified in the CCSKs with either *BCOR* ITD or *YWHAE* fusion and in *BCOR-CCNB3*-positive round cell sarcoma from the published data (Fig. 5B). In contrast to *CIC-DUX4*-positive sarcomas, *ETV1, ETV4* and *ETV5* mRNA expressions were not upregulated in *BCOR*-ITD URCS/PMMTI (data not shown).

The Gene Signature of *BCOR* ITD–positive URCS/PMMTI Shows Significant Overlap With CCSK and *BCOR-CCNB3*-positive Sarcoma

By unsupervised clustering, the URCS and PMMTI with *BCOR* ITD grouped together in a distinct cluster from other sarcomas (Fig. 3B). The *YWHAE-NUTM2B* fusion–positive URCS also clustered together with the *BCOR* ITD URCS (Fig. 3B). A gene list of 404 differentially expressed genes was obtained as the *BCOR* ITD gene signature of URCS and PMMTI based on our RNAseq data. From the publicly available CCSK data set, we obtained a 359 differentially expressed gene list compared with normal kidney. Comparing the gene signature of CCSK with that of *BCOR* ITD–positive URCS/PMMTI, we identified 119 (33%) overlapping genes (Fig. 5A). Among them, 44 genes were also upregulated in the *BCOR-CCNB3* fused round cell sarcoma (Fig. 5A). The GSEA algorithm showed significant enrichment (FDR < 0.25) of this 44 gene list across the 3 tumor data sets obtained from different platforms (Fig. 5A). Hierarchical clustering using the same 44 gene list showed a distinct cluster of *BCOR* ITD–positive URCS/PMMTI from other sarcomas. In addition, the *YWHAE-NUTM2B* and *BCOR-MAML3* fusion–positive URCS also grouped with *BCOR* ITD–positive URCS. Similarly, in the CCSK cohort, the 2 *YWHAE-NUTM2B/E*-positive cases grouped together with *BCOR* ITD–positive tumors and separate from the non-neoplastic kidney samples. Furthermore, using this common gene list, the *BCOR-CCNB3*-positive sarcomas grouped together but separate from the Ewing sarcomas and normal tissues. Expression levels of representative upregulated genes from the 44 gene list, including *BCOR*, *ZIC2*, *PITX1*, *LHX2*, *SATB2*, and *KDM2B*, are shown in Figure 5B.

Upon review, there was also a morphologic overlap noted among *BCOR* ITD–positive URCS/PMMTI, CCSK, and URCS with *BCOR-MAML3* and *BCOR-CCNB3* fusion (Fig. 6). The tumor nuclei showed homogenous fine chromatin pattern, lacking prominent nucleoli. The delicate vascular network was also observed in our control cases of CCSK (Fig. 6A) and *BCOR-MAML3* URCS (Fig. 6B). Some areas of myxoid stromal change and more oval to short spindling tumor cells were also seen in *BCOR-CCNB3* sarcoma.

DISCUSSION

Infantile/congenital sarcomas with a round cell phenotype are uncommon and often diagnostically challenging. In contrast to the spindle cell sarcomas that frequently occur in this age group, such as *ETV6-NTRK3* fusion–positive infantile fibrosarcoma[20] and less commonly congenital spindle cell rhabdomyosarcoma with *VGLL2*-related fusions,[21] most of the well-established round cell sarcoma entities, such as Ewing sarcoma, desmoplastic round cell sarcoma, or sarcomas with *CIC-DUX4* or *BCOR-CCNB3* fusions rarely occur in infants.[16,22–28] In fact, in our database of 31 infantile round cell sarcomas occurring in soft tissue, only 2 (6.5%) cases had known gene fusions (one *EWSR1-ERG*, the other *EWSR1-ETV4*). With relatively nonspecific histomorphology and largely unknown genetic abnormalities, many of these cases thus fall into the category of URCS.

Interestingly, CCSK is also a sarcoma with round cell phenotype, which almost always occurs in the kidneys of young children, with an age range at diagnosis between 2 months and 14 years, with a mean of 36 months and a median of 30 months.[2] The genetic hallmark of CCSK was characterized recently as either harboring *BCOR*-ITD in most cases[7] or a *YWHAE-NUTM2B/E* fusion in 12% of cases,[8] molecular abnormalities which appear to be mutually exclusive.[9] Rare cases of extrarenal CCSK have been reported, including 3 infants with tumors involving soft tissue of the neck,[5] terminal ileum,[4] and ovary,[2,3] respectively, and 2 teenagers (13 and 11 y old) with tumors involving pelvic cavity[2,6] and retroperitoneum,[2] respectively. To our knowledge, only the neck mass of a 3-week-old boy, which was histologically similar to CCSK, was reported to harbor a *YWHAE-NUTM2B/E* fusion,[5] whereas the fusion status of other extrarenal CCSK cases are unknown. No *BCOR* ITD data have been reported to date on extrarenal CCSK or soft tissue sarcomas.

In this study, we identified a *YWHAE-NUTM2B* fusion in 2 (9%) and *BCOR* ITD in 9 (41%) cases of 22 infantile URCS of soft tissue studied. There were 7 boys and 4 girls, with an age range of 8 days to 11 months. The tumors occurred preferentially in the soft tissue of trunk, pelvis/retroperitoneum, and head and neck, sparing the

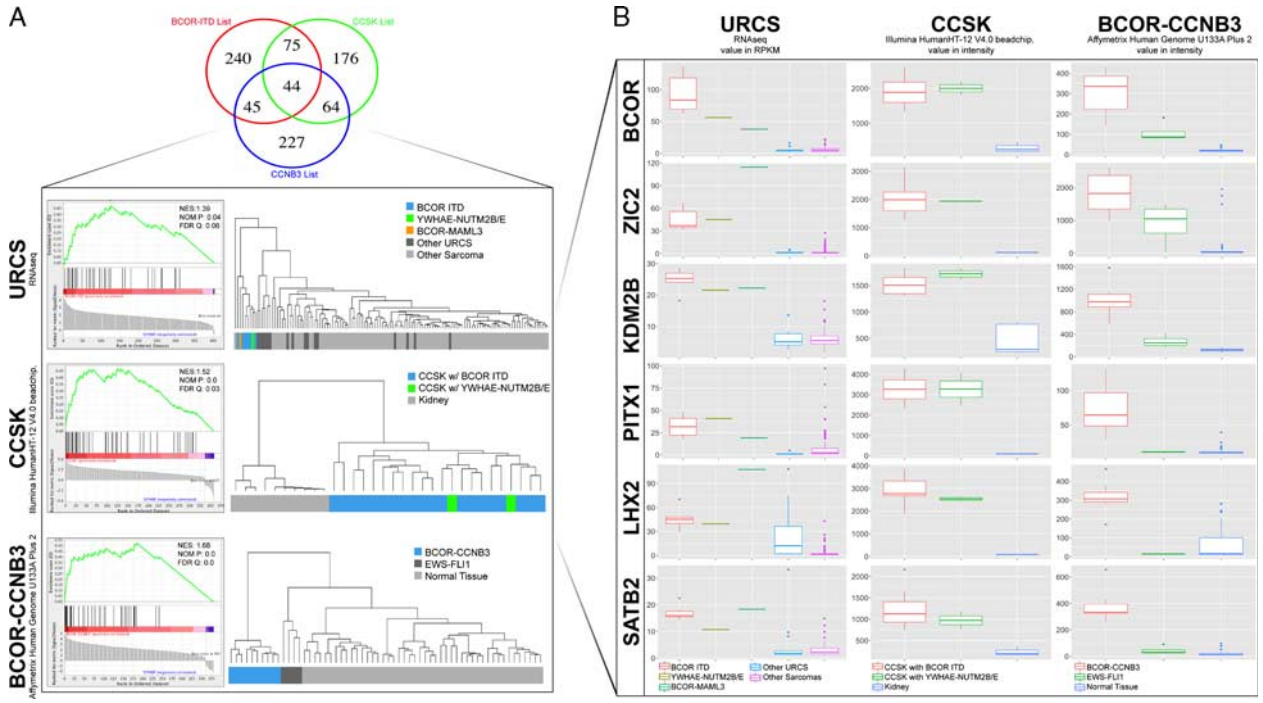

FIGURE 5. URCS/PMMTI with *BCOR* ITD display overlapping gene signature with CCSK and *BCOR-CCNB3*-positive sarcoma. A, Venn diagram showing overlapping differential gene signature between *BCOR* ITD URCS (RNA-seq data), CCSK (published data, Illumina HumanHT-12 V4.0 beadchip platform),[15] and round cell sarcoma with *BCOR-CCNB3* (published data, Affymetrix Human Genome U133A Plus 2 platform).[16] The GSEA analysis demonstrates enrichment of the 44 genes in common among the 3 tumor categories. Subsequent supervised hierarchical clustering using this 44 gene list revealed that *BCOR* ITD–positive and *YWHAE* fusion–positive tumors grouped together, separate from the control groups. B, Comparative expression of commonly upregulated genes: *BCOR*, *ZIC2*, *KDM2B*, *PITX1*, *LHX2*, and *SATB2*, across these 3 tumor entities and individual platforms (URSC with *BCOR* ITD, *YWHAE-NUTM2B*, *BCOR-MAML3* on RNAseq; *BCOR* ITD and *YWHAE-NUTM2B/E* CCSK on Illumina HumanHT-12 V4.0 beadchip platform[15]; and round cell sarcoma with *BCOR-CCNB3* on Affymetrix Human Genome U133A Plus 2 platform).[16] NES indicates normalized enrichment score; NOM P, nominal *P*-value; other URCS, URCS without known genetic alterations.

extremities. Our results are in keeping with prior observations that the presence of *BCOR* ITD and *YWHAE-NUTM2B/E* fusions are mutually exclusive molecular events in URCS as they are in CCSK.[9] URCS with these 2 genetic abnormalities share similar histologic features as well as significant overlap with the wide morphologic spectrum of CCSK.[2] As seen in the classic pattern of CCSK, many of these soft tissue URCSs were composed of a proliferation of uniform round cells with open chromatin and a delicate arborizing capillary network. In addition, the less common patterns described in CCSK, such as myxoid pattern or epithelioid pattern with acinar or rosette-like structures,[2] were also seen in the *BCOR-ITD/YWHAE*-positive soft tissue URCS. In the pathologic studies before the identification of these genetic abnormalities, the classic histologic pattern was noted in >90% of renal CCSKs at least focally.[2] In the present soft tissue cohort of infantile URCS, the "classic CCSK pattern" was seen in 5/11 (45%) cases harboring either a *YWHAE* rearrangement or *BCOR* ITD. No distinct

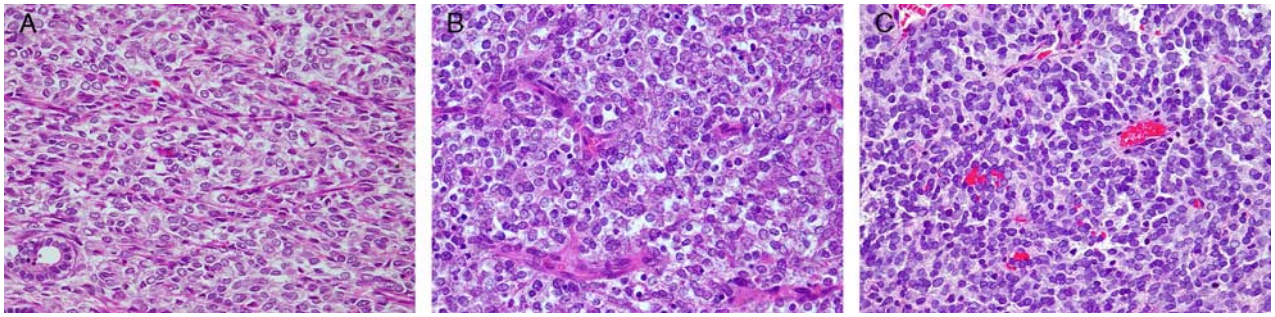

FIGURE 6. Histologic overlap among CCSK and URCS with *BCOR* ITD and other *BCOR*-related fusions. A similar cytomorphology with fine chromatin and delicate vascular network in CCSK (A), *BCOR-MAML3* URCS (B), and *BCOR-CCNB3* URCS (C).

morphologic features were noted in the infantile soft tissue URCS lacking both genetic abnormalities.

Interestingly, *BCOR* ITDs were also identified in the majority of cases diagnosed as PMMTI (6/7, 86%). Initially classified among infantile fibrosarcomas due to overlapping histology and demographics, PMMTI was subsequently recognized as a distinct entity of possible fibroblastic-myofibroblastic derivation on the basis of its lack of *ETV6-NTRK3* genetic abnormality, distinctive primitive cells, myxoid background, and a more locally aggressive clinical behavior compared with infantile fibrosarcoma.[10] The largest series of PMMTI reported to date encompassed 6 cases, with a narrow age range of 0 to 2 months old and a wide anatomic distribution, including trunk, extremity, and head and neck.[10] All except 1 of their patients with available clinical information had local recurrence or persistent disease, but most were still alive at the last follow-up. Histologically, the tumors were described as having a myxoid background, delicate vascular network, and primitive spindle, polygonal to round tumor cells. Focal short spindle cell fascicles may also be seen. Aside from the soft tissue location, PMMTI shares some clinicopathologic overlap with CCSK. In this study, we included 2 cases (cases 1 and 4) from the initial PMMTI cohort[10] and 4 additional cases diagnosed as PMMTI. Similar to URCS cases, *BCOR* ITD was only identified in PMMTI occurring in patients under the age of 1 year (2 to 10 mo old), with the tumors presenting in the soft tissue of trunk, abdominal cavity/retroperitoneum, and rarely head and neck. On the basis of these overlapping clinicopathologic features, we propose that PMMTI and a subset of infantile URCS might represent the soft tissue counterpart of CCSK.

Although our study included a large cohort of soft tissue URCS, spanning a wide age range (infants, older children, adolescents, adults), the 2 genetic abnormalities—*YWHAE-NUTM2B* fusion and *BCOR* ITD—were found exclusively in infants. None of the older patients with URCS studied (range, 3 to 29 y) had *BCOR* ITD or *YWHAE* rearrangements. Moreover, the only case of extrarenal CCSK with a reported *YWHAE-NUTM2B/E* fusion occurred also in a 3-week-old infant.[5] This finding is intriguing, as renal CCSK harboring similar genetic abnormalities show a broader age range at diagnosis: 0 to 9 years for the *BCOR* ITD–positive cases[7,9,18,19] and 0.5 to 6 years in *YWHAE*-rearranged CCSK.[8,29]

Similar to CCSK, the duplicated *BCOR* sequences were all in-frame and consistently located in the last exon of *BCOR*, although they were variable in the number of nucleotides and the genomic positions. Comparing the spectrum of *BCOR* ITD variants seen in soft tissue URCS/PMMTI, there were a number of them similar to the ones described in renal CCSK[7,9,18,19] but also several novel ITD variants, with a wider size range (63 to 120 bp). The common duplicated region of 13 amino acids previously described in CCSK was also present in all of our *BCOR* ITD variants.[7]

BCOR (BCL-6 interacting corepressor) was first described to interact with BCL-6 POZ domain through its BCOR BCL6-binding domain and potentiate the transcriptional repression of BCL-6.[30,31] BCOR is also part of a subtype of polycomb repressive complex 1 (PRC1), together with PCGF1, RING1B, and KDM2B. In this complex, the PUFD (PCGF Ub-like fold discriminator) domain of BCOR, located at the C terminus, binds to PCGF1 (polycomb-group RING finger homologue 1), (Fig. 3A).[32,33] This BCOR complex, categorized as a noncanonical PRC1 complex, regulates gene transcription through an epigenetic silencing mechanism. It is recruited to nonmethylated CpG islands and catalyzes demethylation of H3K36me2 and monoubiquitylation of H2AK119.[34] It has been shown to play a role in embryonic stem cell differentiation and the regulation of mesenchymal stem cell function.[35,36]

Genetic alterations in *BCOR* have been reported in several human diseases. Germline *BCOR* loss of function mutations (truncation, frameshift) result in X-linked oculofaciocardiodental syndromes, presenting with congenital cataracts, dysmorphic facies, cardiac abnormalities, radiculomegaly, and associated with male lethality.[37] In cancer, somatic mutations of *BCOR* have been detected in a small subset of acute myeloid leukemia, myelodysplastic syndrome, and chronic myelomonocytic leukemia.[34] Chromosomal rearrangements involving *BCOR* have also been found in round cell sarcomas (*BCOR-CCNB3*; *BCOR-MAML3*),[11,16] endometrial stromal sarcoma and ossifying fibromyxoid tumor (*ZC3H7B-BCOR*),[38,39] and acute myeloid leukemia (*BCOR-RARα*).[40] In CCSK and infantile round cell sarcoma with *BCOR* ITD, the ITD sequences located at the C-terminal may affect the PUFD domain conformation of the BCOR protein. The additional stretch of amino acids (ITD) in the PUFD domain might interfere with PCGF1 binding and thus could affect the PRC1-related epigenetic modifications; although the exact mechanism remains to be investigated.

A high *BCOR* mRNA expression, spanning the entire transcript rather than restricted to the exon 16 ITD region, was identified in all *BCOR* ITD–positive URCS and PMMTI cases, as previously documented in CCSK.[7,18,19] Furthermore, *BCOR* upregulation was also detected in our *YWHAE-NUTM2B* fusion–positive URCS, similar to the 2 previously reported fusion-positive CCSK cases.[9] These results suggest that despite the 2 different genetic abnormalities seen in URCS, PMMTI, and CCSK spectrum, a common core of *BCOR* mRNA overexpression is present, which may trigger a similar downstream pathway. Moreover, transcriptional *BCOR* upregulation was also found in the *BCOR-MAML3* and *BCOR-CCNB3* round cell sarcomas.[11,16] These findings suggest different mechanisms of *BCOR* overexpression, either through conventional gene fusions or ITD, and may emerge as a critical molecular event in these URCSs. In addition to *BCOR* upregulation, URCS/PMMTI and CCSK further shared a significant transcriptional signature resulting in a tight clustering pattern of URCS/PMMTI and CCSK, respectively, from their appropriate control groups. Of interest, *BCOR-CCNB3* round cell

sarcoma also shared a transcriptional profile similar to *BCOR* ITD neoplasia. In light of these findings, we observed in retrospect certain histologic overlap between our *BCOR* ITD–positive soft tissue URCS and other URCSs with *BCOR*-related gene fusions. In contrast to classic Ewing sarcoma and *CIC-DUX4* fusion–positive URCS, *BCOR-CCNB3*[27,41] and *BCOR-MAML3*[11] fusion–positive tumors more often display an oval to spindle cell phenotype, with myxoid areas, thus showing overlapping morphologic features with *BCOR* ITD infantile URCS and renal CCSK tumors. Furthermore, the limited data available on patients with *BCOR-CCNB3* tumors suggests that the clinical behavior might be less aggressive than other Ewing sarcoma family of tumors.[27] In contrast to the *CIC-DUX4*-positive sarcomas, *BCOR* ITD–positive and *YWHAE*-rearranged URCS did not show upregulation of the PEA3 family of transcription factors, including *ETV1*, *ETV4*, and *ETV5*.[42] However, further investigations including functional studies are required to assess more definitively the pathogenetic link between these pathologic entities sharing *BCOR* mRNA overexpression.

In conclusion, we report 17 cases of infantile URCS/PMMTI with identical genetic abnormalities to CCSK, including either ITD in the last exon of *BCOR* or *YWHAE-NUTM2B* fusion. Moreover, our results show a significant demographic and morphologic overlap between this subset of URCS in infants, PMMTI and CCSK, suggesting a single disease entity affecting this age group. Our results also raise the possibility of further genetic links with other *BCOR* fusion–related sarcomas (ie, *BCOR-MAML3* and *BCOR-CCNB3*). Our data also suggest that the detection of *BCOR*-ITD by PCR or *YWHAE* gene rearrangement by FISH can be used in clinical practice for confirming this diagnosis in challenging cases of soft tissue tumors in infants. Further investigations are needed to evaluate the biological behavior of these patients, as our study had very limited clinical follow-up. Moreover, larger studies are also required to investigate the appropriate therapeutic modalities for this genetically distinct group of tumors and whether they could benefit from the current intensive treatment protocol, which has improved the prognosis for CCSK.[2,43,44]

REFERENCES

1. Fletcher C, Bridge JA, Hogendoorn PC, et al. *WHO Classification of Tumours of Soft Tissue and Bone*. Lyon: IARC; 2013.
2. Argani P, Perlman EJ, Breslow NE, et al. Clear cell sarcoma of the kidney: a review of 351 cases from the National Wilms Tumor Study Group Pathology Center. *Am J Surg Pathol*. 2000;24:4–18.
3. Finn LS, Patterson K. Ovarian sarcoma with pathologic features of clear cell sarcoma of the kidney. *Pediatr Dev Pathol*. 2000;3:487–491.
4. Kataoka Y, Shimada H, Sugimoto T, et al. Congenital sarcoma in the terminal ileum histologically resembling clear cell sarcoma of the kidney: a case report with an immunohistochemical study. *Hum Pathol*. 1993;24:1026–1030.
5. Fehr A, Hansson MC, Kindblom LG, et al. YWHAE-FAM22 gene fusion in clear cell sarcoma of the kidney. *J Pathol*. 2012;227:e5–e7.
6. Weeks DA, Malott RL, Zuppan C, et al. Primitive pelvic sarcoma resembling clear cell sarcoma of kidney. *Ultrastruct Pathol*. 1991;15:403–408.
7. Ueno-Yokohata H, Okita H, Nakasato K, et al. Consistent in-frame internal tandem duplications of BCOR characterize clear cell sarcoma of the kidney. *Nat Genet*. 2015;47:861–863.
8. O'Meara E, Stack D, Lee CH, et al. Characterization of the chromosomal translocation t(10;17)(q22;p13) in clear cell sarcoma of kidney. *J Pathol*. 2012;227:72–80.
9. Karlsson J, Valind A, Gisselsson D. BCOR internal tandem duplication and YWHAE-NUTM2B/E fusion are mutually exclusive events in clear cell sarcoma of the kidney. *Genes Chromosomes Cancer*. 2016;55:120–123.
10. Alaggio R, Ninfo V, Rosolen A, et al. Primitive myxoid mesenchymal tumor of infancy: a clinicopathologic report of 6 cases. *Am J Surg Pathol*. 2006;30:388–394.
11. Specht K, Zhang L, Sung YS, et al. Novel BCOR-MAML3 and ZC3H7B-BCOR gene fusions in undifferentiated small blue round cell sarcomas. *Am J Surg Pathol*. 2016. DOI: 10.1097/PAS.0000000000000591. (In Press).
12. Dobin A, Davis CA, Schlesinger F, et al. STAR: ultrafast universal RNA-seq aligner. *Bioinformatics*. 2013;29:15–21.
13. Kim D, Pertea G, Trapnell C, et al. TopHat2: accurate alignment of transcriptomes in the presence of insertions, deletions and gene fusions. *Genome Biol*. 2013;14:R36.
14. Mortazavi A, Williams BA, McCue K, et al. Mapping and quantifying mammalian transcriptomes by RNA-Seq. *Nat Methods*. 2008;5:621–628.
15. Karlsson J, Holmquist Mengelbier L, Ciornei CD, et al. Clear cell sarcoma of the kidney demonstrates an embryonic signature indicative of a primitive nephrogenic origin. *Genes Chromosomes Cancer*. 2014;53:381–391.
16. Pierron G, Tirode F, Lucchesi C, et al. A new subtype of bone sarcoma defined by BCOR-CCNB3 gene fusion. *Nat Genet*. 2012;44:461–466.
17. Richter GH, Plehm S, Fasan A, et al. EZH2 is a mediator of EWS/FLI1 driven tumor growth and metastasis blocking endothelial and neuro-ectodermal differentiation. *Proc Natl Acad Sci USA*. 2009;106:5324–5329.
18. Astolfi A, Melchionda F, Perotti D, et al. Whole transcriptome sequencing identifies BCOR internal tandem duplication as a common feature of clear cell sarcoma of the kidney. *Oncotarget*. 2015;6:40934–40939.
19. Roy A, Kumar V, Zorman B, et al. Recurrent internal tandem duplications of BCOR in clear cell sarcoma of the kidney. *Nat Commun*. 2015;6:8891.
20. Minard-Colin V, Orbach D, Martelli H, et al. [Soft tissue tumors in neonates]. *Arch Pediatr*. 2009;16:1039–1048.
21. Alaggio R, Zhang L, Sung YS, et al. A Molecular Study of Pediatric Spindle and Sclerosing Rhabdomyosarcoma: Identification of Novel and Recurrent VGLL2-related Fusions in Infantile Cases. *Am J Surg Pathol*. 2016;40:224–235.
22. Maygarden SJ, Askin FB, Siegal GP, et al. Ewing sarcoma of bone in infants and toddlers. A clinicopathologic report from the Intergroup Ewing's Study. *Cancer*. 1993;71:2109–2118.
23. Jinkala SR, Basu D, Mathath D, et al. A rare case of congenital Ewing sarcoma/PNET of the scapula. *J Pediatr Hematol Oncol*. 2014;36:e134–e135.
24. Salgado C, Neff T, Frazier L, et al. An unusual case of congenital primitive neuroectodermal tumor with ocular metastasis. *J Pediatr Hematol Oncol*. 2012;34:e69–e71.
25. Choi EY, Thomas DG, McHugh JB, et al. Undifferentiated small round cell sarcoma with t(4;19)(q35;q13.1) CIC-DUX4 fusion: a novel highly aggressive soft tissue tumor with distinctive histopathology. *Am J Surg Pathol*. 2013;37:1379–1386.
26. Cohen-Gogo S, Cellier C, Coindre JM, et al. Ewing-like sarcomas with BCOR-CCNB3 fusion transcript: a clinical, radiological and pathological retrospective study from the Societe Francaise des Cancers de L'Enfant. *Pediatr Blood Cancer*. 2014;61:2191–2198.

27. Puls F, Niblett A, Marland G, et al. BCOR-CCNB3 (Ewing-like) sarcoma: a clinicopathologic analysis of 10 cases, in comparison with conventional Ewing sarcoma. *Am J Surg Pathol*. 2014;38:1307–1318.
28. Gerald WL, Ladanyi M, de Alava E, et al. Clinical, pathologic, and molecular spectrum of tumors associated with t(11;22)(p13;q12): desmoplastic small round-cell tumor and its variants. *J Clin Oncol*. 1998;16:3028–3036.
29. Karlsson J, Lilljebjorn H, Holmquist Mengelbier L, et al. Activation of human telomerase reverse transcriptase through gene fusion in clear cell sarcoma of the kidney. *Cancer Lett*. 2015;357:498–501.
30. Huynh KD, Fischle W, Verdin E, et al. BCoR, a novel corepressor involved in BCL-6 repression. *Genes Dev*. 2000;14:1810–1823.
31. Ghetu AF, Corcoran CM, Cerchietti L, et al. Structure of a BCOR corepressor peptide in complex with the BCL6 BTB domain dimer. *Mol Cell*. 2008;29:384–391.
32. Junco SE, Wang R, Gaipa JC, et al. Structure of the polycomb group protein PCGF1 in complex with BCOR reveals basis for binding selectivity of PCGF homologs. *Structure*. 2013;21:665–671.
33. Gearhart MD, Corcoran CM, Wamstad JA, et al. Polycomb group and SCF ubiquitin ligases are found in a novel BCOR complex that is recruited to BCL6 targets. *Mol Cell Biol*. 2006;26:6880–6889.
34. Yamamoto Y, Abe A, Emi N. Clarifying the impact of polycomb complex component disruption in human cancers. *Mol Cancer Res*. 2014;12:479–484.
35. Wamstad JA, Corcoran CM, Keating AM, et al. Role of the transcriptional corepressor Bcor in embryonic stem cell differentiation and early embryonic development. *PLoS One*. 2008;3:e2814.
36. Fan Z, Yamaza T, Lee JS, et al. BCOR regulates mesenchymal stem cell function by epigenetic mechanisms. *Nat Cell Biol*. 2009;11:1002–1009.
37. Ng D, Thakker N, Corcoran CM, et al. Oculofaciocardiodental and Lenz microphthalmia syndromes result from distinct classes of mutations in BCOR. *Nat Genet*. 2004;36:411–416.
38. Antonescu CR, Sung YS, Chen CL, et al. Novel ZC3H7B-BCOR, MEAF6-PHF1, and EPC1-PHF1 fusions in ossifying fibromyxoid tumors–molecular characterization shows genetic overlap with endometrial stromal sarcoma. *Genes Chromosomes Cancer*. 2014;53:183–193.
39. Panagopoulos I, Thorsen J, Gorunova L, et al. Fusion of the ZC3H7B and BCOR genes in endometrial stromal sarcomas carrying an X;22-translocation. *Genes Chromosomes Cancer*. 2013;52:610–618.
40. Yamamoto Y, Tsuzuki S, Tsuzuki M, et al. BCOR as a novel fusion partner of retinoic acid receptor alpha in a t(X;17)(p11;q12) variant of acute promyelocytic leukemia. *Blood*. 2010;116:4274–4283.
41. Peters TL, Kumar V, Polikepahad S, et al. BCOR-CCNB3 fusions are frequent in undifferentiated sarcomas of male children. *Mod Pathol*. 2015;28:575–586.
42. Specht K, Sung YS, Zhang L, et al. Distinct transcriptional signature and immunoprofile of CIC-DUX4 fusion-positive round cell tumors compared to EWSR1-rearranged Ewing sarcomas: further evidence toward distinct pathologic entities. *Genes Chromosomes Cancer*. 2014;53:622–633.
43. Furtwangler R, Gooskens SL, van Tinteren H, et al. Clear cell sarcomas of the kidney registered on International Society of Pediatric Oncology (SIOP) 93-01 and SIOP 2001 protocols: a report of the SIOP Renal Tumour Study Group. *Eur J Cancer*. 2013;49:3497–3506.
44. Gooskens SL, Furtwangler R, Vujanic GM, et al. Clear cell sarcoma of the kidney: a review. *Eur J Cancer*. 2012;48:2219–2226.